iScience, Volume *26*

Supplemental information

The regulatory mechanism of the yeast osmoresponse under different glucose concentrations

Wenting Shen, Ziqing Gao, Kaiyue Chen, Alusi Zhao, Qi Ouyang, and Chunxiong Luo

Table S1 Parameter settings, Related to Figure 4.

k_1	5
k_g	0.25
k_2	100
k_{p1}	100
k_{p2}	100
k_h	0.05
k_{h2}	0.001
k_r	0.07
k_s	100
c_0	50
c_m	50
Δc	40
a_1	0.001
a_2	1
a_3	1
a_4	0.005
a_5	0.5
$a_{5'}$	0.001
a_6	0.1
a_7	0.1
a_8	0.4
a_9	0.05
a_{10}	0.1
a_{11}	0.2
a_{12}	0.1
b_{GB}	300

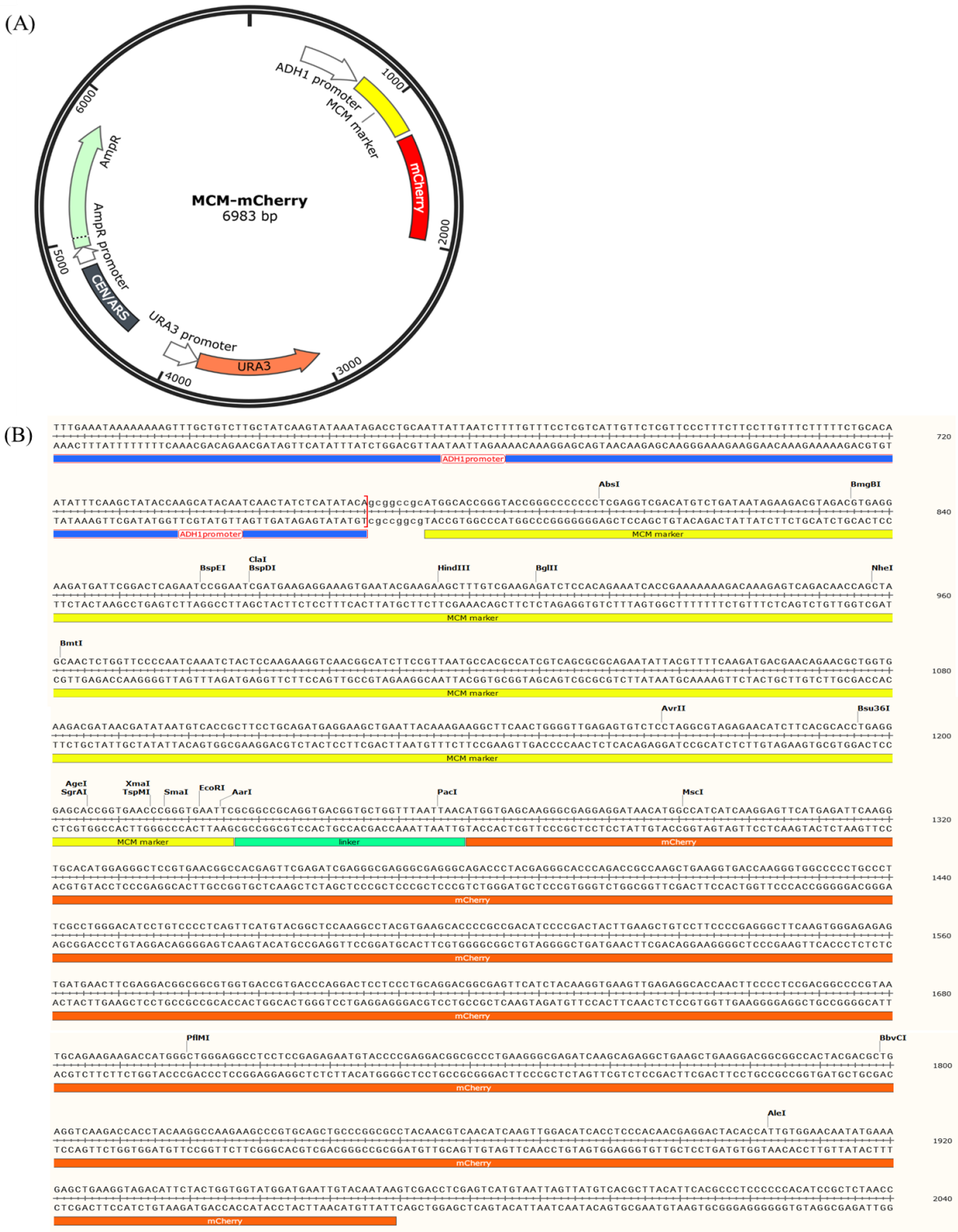

Figure S1. Mcm-mCherry Plasmid, Related to Figure 1

(A) Map of plasmid of Mcm-mCherry (6983 bp).

(B) Detailed sequence of the multiple cloning site of Mcm-mCherry.

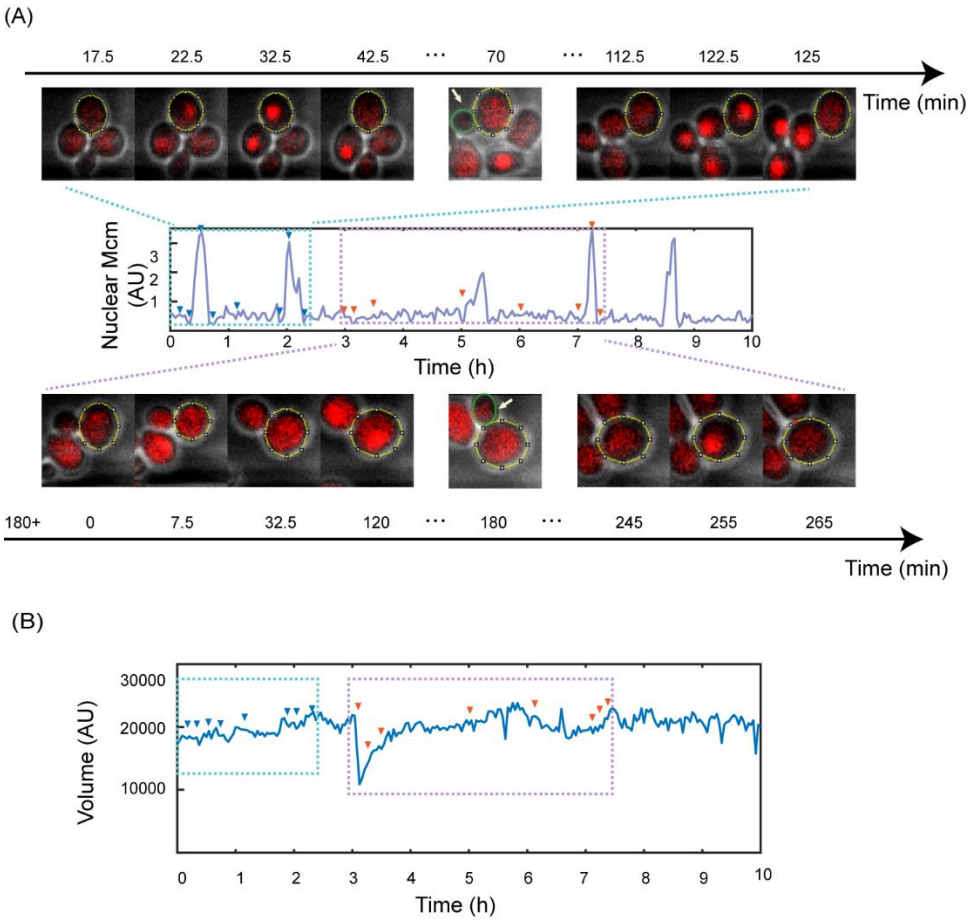

Figure S2. Cellular physiology, Related to Figure 1

(A) Snapshot from a time-lapse movie of cells showing Mcm nuclear localization. The yellow circles trace an example of a single cell, and the triangles indicate the times cells enter the G1 phase. The two cycles before and after the stimulus are magnified. The arrow marks the bud from the cell.

(B Volume of the individual cells highlighted above. The triangle corresponds to the moment in Figure S1 A.

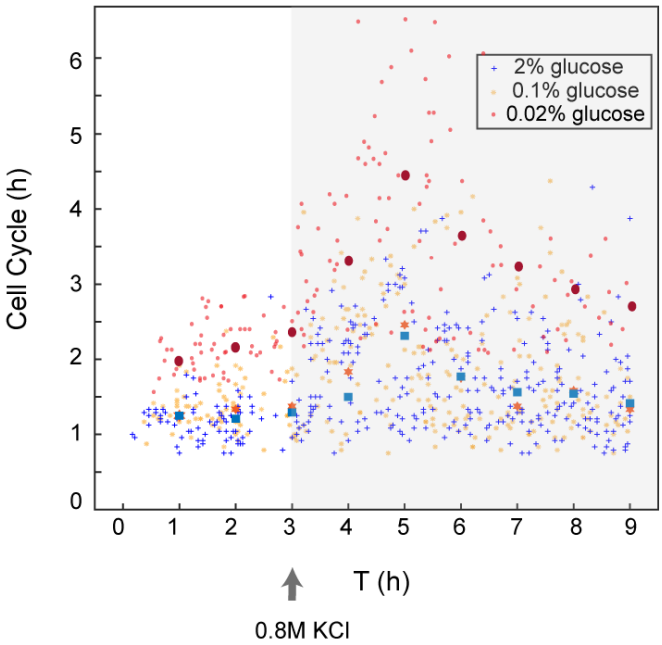

Figure S3. Cell cycle in single cells, Related to Figure 1

Sustained hyperosmotic stress was induced at 3 hours. The X-axis indicates the midpoint of the two G1 phases. The highlighted orange star (0.1%), blue square (2%) and red circle (0.02%) indicate the median value of the cell cycle in single cells during the previous hour.

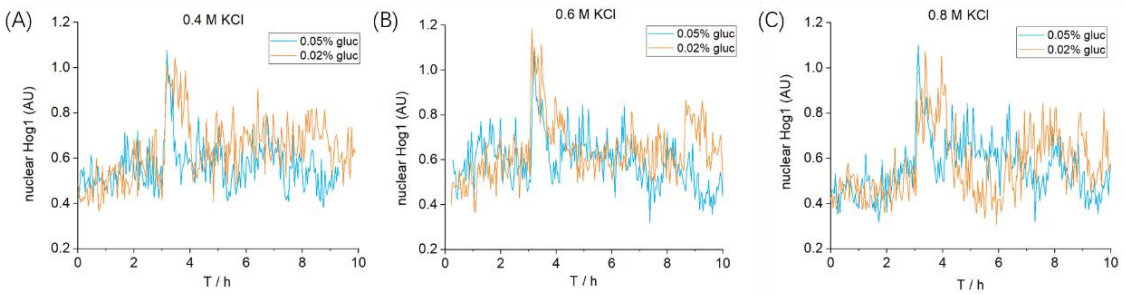

Figure S4 Hog1 nuclear localization, Related to Figure 2.

Localization trajectory of Hog1 in typical cells when the duration of Hog1 was at the median of the population. Cells were cultured in 0.02% and 0.05% glucose environments, and 0.4 M (A), 0.6 M (B), and 0.8 M (C) KCl were added at 3 hours.

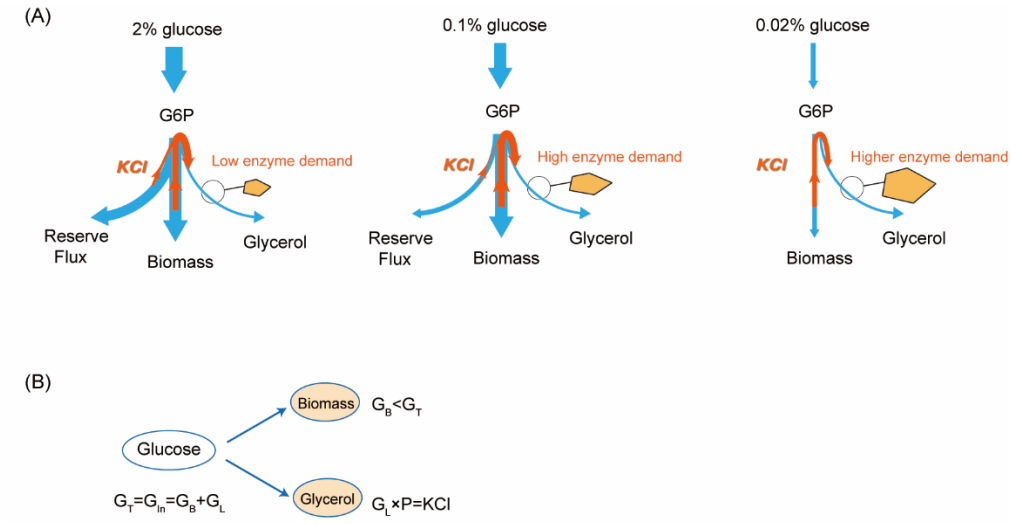

Figure S5. Glycolytic allocation strategy under different glucose concentrations, Related to Figure 3

(A) Metabolic reconfiguration strategy in yeast. When glucose is limited, cells preferentially route the glycolytic flux to biosynthesis and maximize current growth, saving the cost of a defense reserve flux (middle panel). When glucose decreases further such that the maximum growth rate cannot be maintained (<0.1%), there is no excess glycolysis available for a defensive reserve flux (right panel). After exposure to osmostress, lower flux requires higher expression levels of enzymes for glycerol production.

(B) G_T is the total glycolysis. In a glucose-limited environment (<0.1%) in which a defense reserve flux is abandoned, G_T equals the overall glycolysis input G_{in}. During exposure to osmostress, cells prioritize the stress response. G_L is needed for glycerol production. Enzymatic reactions can be simply considered the product of the substrate and protein concentrations. Due to poor resources, even in the steady state, a continuous glycolytic flux is required for glycerol production. Thus, the carbon required for growth (G_B) cannot be restored to the initial level, which is reflected in the imperfect adaptation of the growth rate.

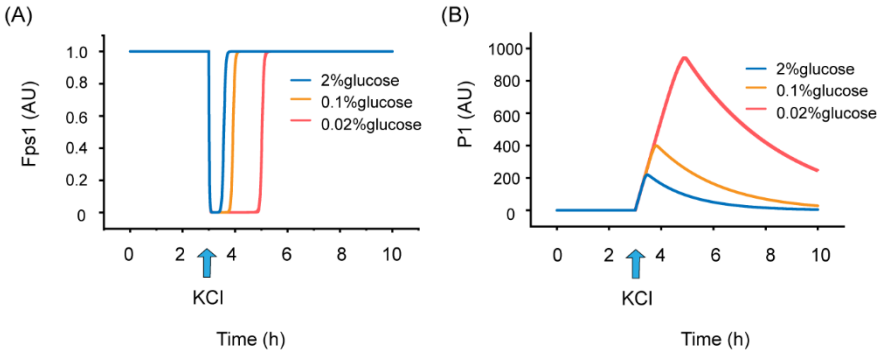

Figure S6 Model predictions of Fps1 and P1, Related to Figure 4.

Model simulation for opened Fps1(nomalized total Fps1 to 1) (A) and P1 (B), following hyperosmotic stress of 0.8 M KCl at 3 h.

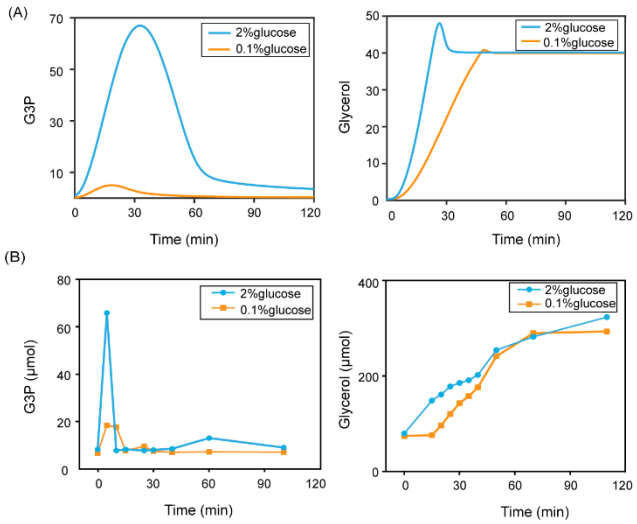

Figure S7. Model predictions and experimental results of metabolites time courses, Related to Figure 4.

A. Model simulation for glycerol-3-phosphate (G3P) and intracellular glycerol.

B. Time courses of G3P and intracellular glycerol following hyperosmotic stress of 0.8 M KCl at time point 0.

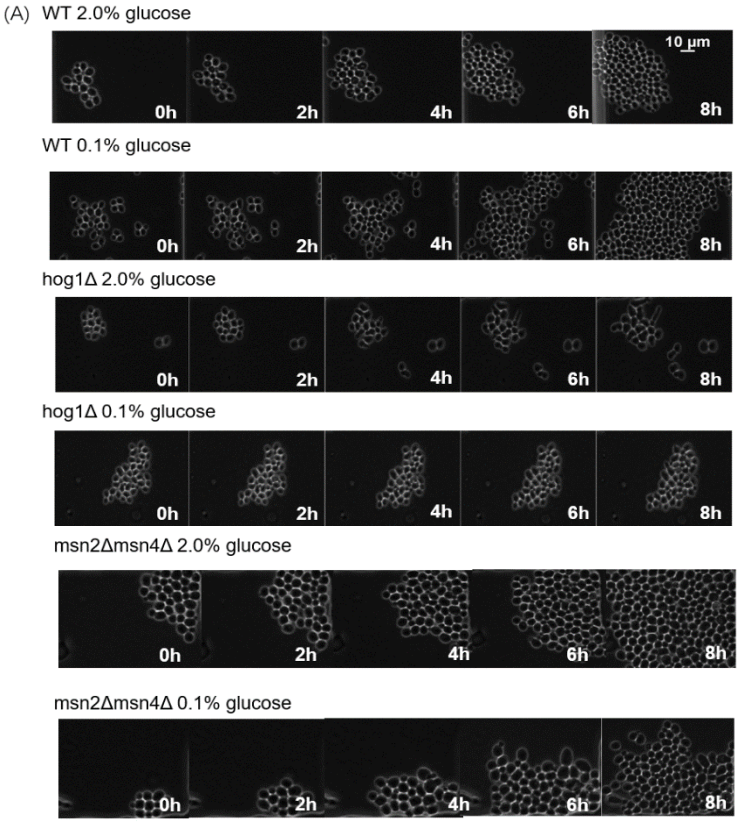

Figure S8. Comparison of different strains upon osmotic stress in 2% and 0.1% glucose environments, Related to Figure 5.

Time course images of different strains under osmotic stress. 0.8 M KCl was added at 0 h

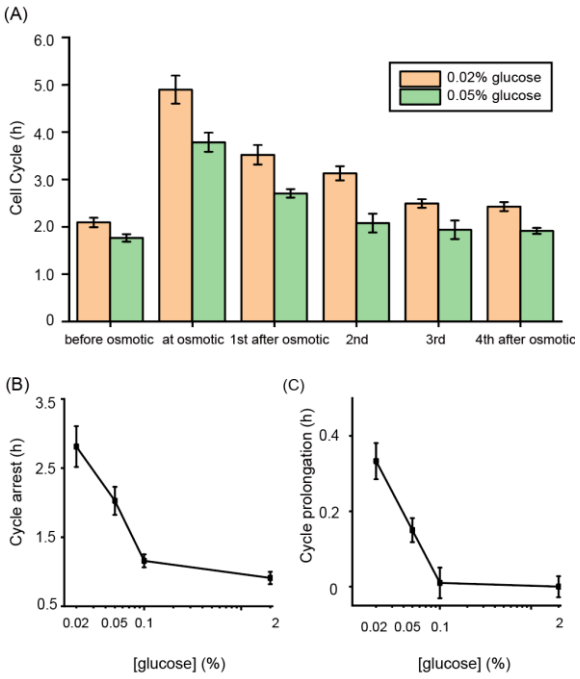

Figure S9. Cell physiological adaptation under different glucose concentrations, Related to Figure 4.

(A) Cell growth phenotype as quantified by the doubling time of untreated cells and after exposure to extracellular 0.8 M KCl. The mean and S.E.M. (N=114 at 0.05%) of the interval duration between the two G1 phases.

(B) Cell cycle arrest after cells were exposed to osmotic stress. Data of 0.02%, 0.1% and 2% glucose are from Figure 2B.

(C) Difference between the steady-state doubling time and the initial value. When the glucose concentration is lower than 0.1%, the fourth cell cycle after the stimulation is considered the steady state. Under the 0.1% and 2% glucose conditions, we used the third cell cycle.

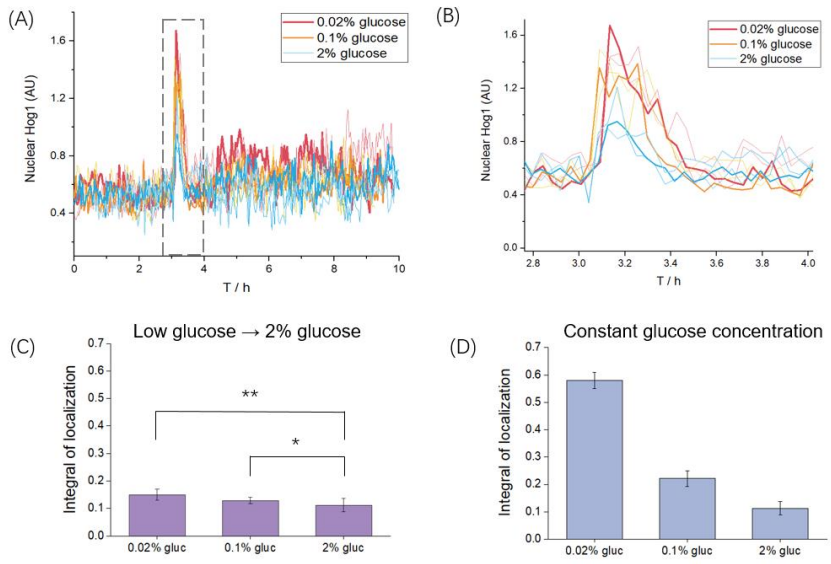

Figure S10. Hog1 translocation under different conditions, Related to Figure 3.

(A) Localization trajectory of the transcriptional regulation of Hog1. Cells were treated with different glucose levels (0.02%, 0.1% and 2%) for 8-9 hours and shifted to 2% glucose with 0.8 M KCl. The bold line is a single cell whose nuclear duration is the median value in the population.

(B) The trajectory of Hog1 at the time of stimulation; a zoomed-in view of Figure S10A.

(C) After switching to 2% glucose and adding 0.8 M KCl, the integral of Hog1 nuclear localization was quantified. Error bars represent the SEM of about 30 cells.

(D) Cells were cultured in 0.02%, 0.1% and 2% constant glucose environments. When exposed to 0.8 M KCl, the integral of Hog1 nuclear localization was quantified. Error bars represent the SEM of about 40 cells

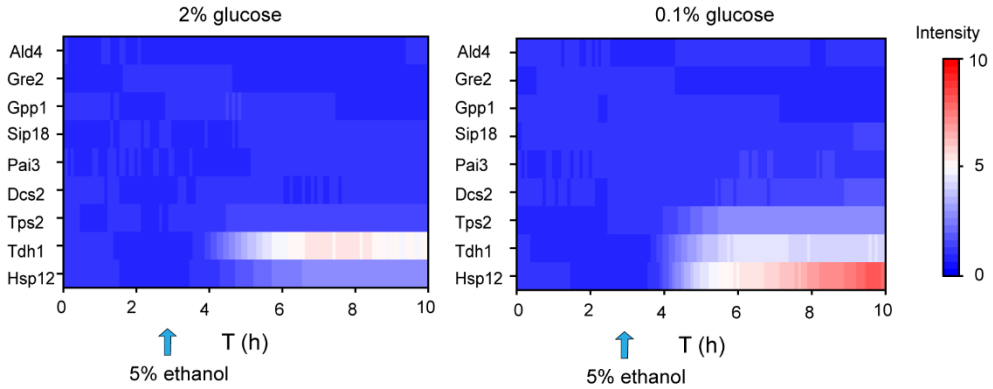

Figure S11. Protein dynamics at different glucose concentrations, Related to Figure 1.

A concentration of 5% ethanol was added at 3 h. The data were normalized to the average protein intensity in the initial 2 hours under 2% glucose, with greater expression indicated by red and lower expression indicated by blue. Among the 9 osmostress-regulated proteins, Hsp12 and Tps2 had stronger response intensities to ethanol stress in a glucose-limited environment (0.1% glucose). The increase in heat shock protein (Hsp12) and trehalose metabolizing enzyme protein (Tps2) expression helps the cell adapt to ethanol stimulation [7,8].